Journal of Hazardous Materials 179 (2010) 49–56

Contents lists available at ScienceDirect

Journal of Hazardous Materials

journal homepage: www.elsevier.com/locate/jhazmat

Photocatalytic degradation of selected herbicides in aqueous suspensions of doped titania under visible light irradiation

Daniela V. Šojić[a], Vesna N. Despotović[a], Nadica D. Abazović[b], Mirjana I. Čomor[b], Biljana F. Abramović[a,*]

[a] Department of Chemistry, Biochemistry and Environmental Protection, Faculty of Sciences, University of Novi Sad, Trg D. Obradovića 3, 21000 Novi Sad, Serbia
[b] Vinča Institute of Nuclear Sciences, 11001 Beograd, PO Box 522, Serbia

ARTICLE INFO

Article history:
Received 27 May 2009
Received in revised form 17 February 2010
Accepted 17 February 2010
Available online 25 February 2010

Keywords:
Fe-doped rutile TiO_2
N-doped anatase TiO_2
Visible light irradiation
Herbicides
Photodegradation
MEP study

ABSTRACT

The aim of this work was to study the efficiency of Fe- and N-doped titania suspensions in the photocatalytic degradation of the herbicides RS-2-(4-chloro-o-tolyloxy)propionic acid (mecoprop, MCPP), (4-chloro-2-methylphenoxy)acetic acid (MCPA), and 3,6-dichloropyridine-2-carboxylic acid (clopyralid, CP) under the visible light ($\lambda \geq 400$ nm) irradiation. The obtained results were compared with those of the corresponding undoped TiO_2 (rutile/anatase) and of the most frequently used TiO_2 Degussa P25. Computational modeling procedures were used to optimize geometry and molecular electrostatic potentials of MCPP, MCPA and CP and discuss the obtained results. The results indicate that the efficiency of photocatalytic degradation is greatly influenced by the molecular structure of the compound. Lowering of the band gap of titanium dioxide by doping is not always favorable for increasing photocatalytic efficiency of degradation.

© 2010 Elsevier B.V. All rights reserved.

1. Introduction

TiO_2 semiconductors that are used in the photocatalysis processes are characterized by a high incidence of recombination between electrons and holes, which unfortunately reduces the efficiency of the photocatalytic process. For an efficient photocatalytic process, it is extremely important to have the charge carriers separated as far as possible, and one of efficient ways for achieving this is the doping of semiconducting materials, such as TiO_2, with various metals and non-metals [1]. Besides, one of the main purposes of such doping is to extend the light absorption edge in order to make use of the majority of the ambient light spectrum. Various computational and experimental methods have proven that the most convenient transition metal for such purposes is iron, due to its ion radius (r_{Ti} = 0.68 Å and r_{Fe} = 0.64 Å) and half-filled electronic configuration [2].

Numerous investigations have shown that the photocatalytic activity of Fe-doped TiO_2 is strongly dependent on the dopant concentration; higher contents of Fe^{3+} result in an increase of the recombination rate of photogenerated electrons and holes and thus in a decrease of the photocatalytic activity [3]. When the iron concentration exceeds an optimal level, the Fe^{3+} ions steadily become the recombination centers of photogenerated electrons and holes. This was ascribed to the fact that more Fe^{3+} sites trap more photogenerated electrons and holes, but the trapped free carrier pairs easily recombine through quantum tunneling [4]. Thus, a higher Fe^{3+} content in the catalyst makes the recombination reaction more probable. Because of that, titania doped with a non-metal, such as carbon [5], sulfur [6], phosphorus [7], fluorine [8], nitrogen [9], etc., which can replace lattice oxygen atoms, are also frequently used for narrowing the band gap of TiO_2. Nitrogen doping can be easily achieved by various methods (sputtering TiO_2 targets in N_2 atmosphere, calcination of TiO_2 in ammonia atmosphere, annealing of TiO_2 with organic compounds containing nitrogen, etc. [9]). Even very low concentrations of nitrogen can produce considerable band gap narrowing of TiO_2 [10]. The properties of doped TiO_2 materials and already mastered synthesis methods [10,11] were the reasons for choosing Fe- and N-doped TiO_2 to study the photocatalytic degradation of herbicides under visible light irradiation. The differences in crystalline structure are inherent to the synthesis procedures – the presence of iron ions makes the rutile structure more stable, and the annealing, as a step in the synthesis of N-doped samples, favors the anatase structure. Besides, in our previous works, we began the study of the efficiency of photocatalytic degradation of selected pesticides under visible light irradiation in aqueous suspensions of TiO_2 Degussa P25 [12] and N-doped anatase TiO_2 (wet synthetic method) [13].

In view of the above, the aim of this work was to investigate the efficiency of Fe-doped rutile TiO_2 [11] and N-doped anatase TiO_2 (dry synthetic method) [10] as photocatalysts in the degradation

* Corresponding author. Tel.: +381 21 4852753; fax: +381 21 454065.
E-mail addresses: daniela.sojic@dh.uns.ac.rs (D.V. Šojić), vesna.despotovic@dh.uns.ac.rs (V.N. Despotović), kiki@vinca.rs (N.D. Abazović), mirjanac@vinca.rs (M.I. Čomor), biljana.abramovic@dh.uns.ac.rs (B.F. Abramović).

0304-3894/$ – see front matter © 2010 Elsevier B.V. All rights reserved.
doi:10.1016/j.jhazmat.2010.02.055

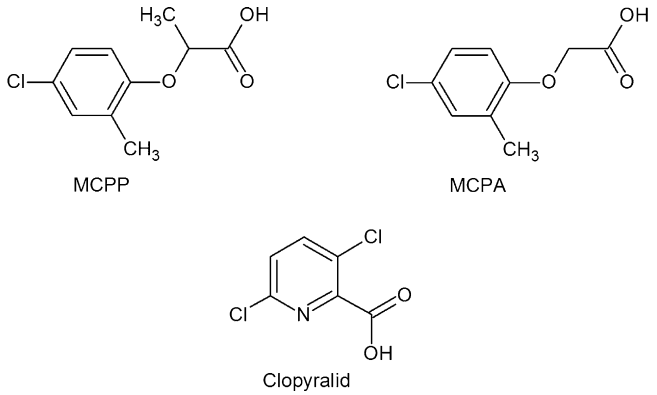

Fig. 1. Structures of the pesticides.

of the herbicides RS-2-(4-chloro-o-tolyloxy)propionic acid (mecoprop, MCPP, $C_{10}H_{11}ClO_3$), (4-chloro-2-methylphenoxy)acetic acid (MCPA, $C_9H_9ClO_3$) and 3,6-dichloropyridine-2-carboxylic acid (clopyralid, CP, $C_6H_3Cl_2NO_2$) (Fig. 1) using visible light ($\lambda \geq 400$ nm) for irradiation. These pesticides were chosen because of their wide use for selective control of many annual and some perennial weeds and because of their frequent presence in drinking water [14,15]. Another important objective was to study how the performance of Fe- and N-doped TiO_2 catalysts compare with that of the corresponding undoped TiO_2 (rutile/anatase) and most frequently used TiO_2 Degussa P25. Finally, the aim was to investigate if the catalyst activity depends on the molecular structure of the compound subjected to photocatalytic degradation. In order to correlate molecular structure of the herbicides with obtained results, we proposed molecular electrostatic potential (MEP) model of these compounds, calculated by Hyperchem 8.0.6.

2. Experimental

2.1. Chemicals and photocatalysts

The commercial herbicide MCPP (98% purity), obtained from the Chemical Factory "Župa" Kruševac, Serbia, was purified by conventional recrystallization from water–ethanol (1:1, v/v) solution, and its purity was checked by ^{1}H NMR spectrometry (Bruker AC-250). MCPA (98.8% purity) and CP (99.4%) were purchased from Riedel-de Haën and used without purification. All other chemicals used were of analytical reagent grade. The herbicides solutions were prepared in doubly distilled water, the initial concentration of MCPP and MCPA being 2.7 mmol dm^{-3} and that of CP 1.0 mmol dm^{-3}.

The Fe-doped rutile TiO_2 powders were synthesized according to a recently described procedure [11]. Briefly, appropriate amount of $FeCl_3$ (Aldrich, p.a.) was dissolved in 200 cm^3 of water. Five cubic centimeters of $TiCl_4$ (Fluka, p.a.) prechilled to −20 °C were added dropwise to the solution containing $FeCl_3$ under stirring. After 2 h of stirring at room temperature, the obtained dispersions were heated and kept at 50 °C for 16 h with constant stirring. The resultant precipitates were dialyzed against water until test reaction for Cl^- was negative, and subsequently dried in vacuum at room temperature. Undoped rutile TiO_2 powder was synthesized in the same manner but without $FeCl_3$. Concentration of Fe^{3+} in TiO_2 matrix was checked by scanning electron microscopy using an energy dispersive spectrometer as detector (SEM/EDS, JEOL JSM-35).

The N-doped anatase TiO_2 powder nanoparticles were obtained by the dry synthetic method [10]. Briefly, freshly prepared $Ti(OH)_4$ dry powder was mixed with urea (1:1 or 1:2; Sigma, p.a.) and heated in the air up to 400 °C for 1 h. Although the stoichiometric content of nitrogen in both N-doped anatase TiO_2 catalysts should be relatively high, the measured content was very low, that is below the detection limit of the X-ray photoelectron spectroscopy (XPS) method, which is reportedly about 1 at.% [16,17]. Undoped anatase TiO_2 powder was synthesized in the same manner but without urea.

The X-ray diffraction (XRD) measurements of the powders were performed on a Philips PW 1710 diffractometer.

The UV/vis diffuse reflectance spectra (DRS) were recorded on an Evolution 600 UV/vis spectrophotometer (Thermo Scientific), equipped with DRA-EV-600 Diffuse Reflectance Accessory.

TiO_2 Degussa P25 (75% anatase and 25% rutile, specific area of 50 m^2 g^{-1}, average particle size 20 nm, non-porous) was used for the purpose of comparison.

FTIR spectra were taken on a Thermo Nicolet Nexus 670 spectrophotometer with 4 cm^{-1} resolution and 100 scans. A volume of 20 cm^3 of 1.0 mmol dm^{-3} CP solution, containing 2000 mg dm^{-3} of the appropriate catalyst, was stirred for 4 h in the dark, to allow herbicide adsorption on TiO_2 particles. The residue obtained after decantation was dried at 60 °C. Spectra were recorded on pellets consisting of a mixture of the sample prepared in this manner and KBr.

All experiments were carried out using a 2000 mg dm^{-3} suspension of the catalyst.

2.2. Photodegradation procedure

Photocatalytic degradation was carried out in a cell described previously [13]. Aqueous suspensions of the catalyst containing herbicide were sonicated for 15 min before irradiation, to make the catalyst particles uniform. The suspension thus obtained was thermostated at 40 ± 0.5 °C in a stream of O_2 and then irradiated with the visible light using a 50 W halogen lamp (Philips) and a 400 nm cut-off filter. The lamp output was calculated to be ca. 1.7×10^{-9} Einstein cm^{-3} min^{-1} (potassium ferrioxalate actinometry). During irradiation, the mixture was stirred at a constant speed. All experiments were carried out at a natural pH (~2.8 for MCPP and MCPA, and 3.2 for CP).

2.3. Analytical procedure

The kinetics of herbicides photodegradation reactions were studied by liquid chromatography–diode array detection (LC–DAD) and UV/vis spectrophotometry.

For the LC–DAD monitoring, aliquots (0.25 cm^3 for MCPP and MCPA, and 0.50 cm^3 for CP, to keep total volume change below 10%) of the reaction mixture were taken at the beginning of the experiment and at regular time intervals. In the case of CP, 5.0 cm^3 of 0.1 mol dm^{-3} HCl were added, and the solution diluted to 10.00 cm^3 with doubly distilled water. The suspensions containing photocatalyst were filtered through Millipore (Millex-GV, 0.22 μm) membrane filter. After that, a 20-μl sample was injected and analyzed on an Agilent Technologies 1100 Series liquid chromatograph, with the UV/vis DAD set at the absorption maxima (228 nm for MCPP and MCPA and 225 nm for CP) and using an Eclypse XDB-C18 (150 mm × 4.6 mm i.d., particle size 5 μm, 25 °C) column. The mobile phase (flow rate 1 cm^3 min^{-1}) was a mixture of acetonitrile and water (1:1, v/v, pH 2.68 for MCPP and MCPA, and 3:7, v/v, pH 2.56 for CP), the water being acidified to make a 0.1% phosphoric acid.

For the spectrophotometric monitoring, samples were prepared in the same way as for LC measurements, and the spectra were recorded in the wavelength range from 200 to 400 nm on a Secomam Anthelie Advanced 2 spectrophotometer in 1 cm quartz cells. The kinetics of herbicides degradation was monitored at 228 nm (MCPP and MCPA) and 225 nm (CP).

Computer modeling procedures used in this study were performed using Hyperchem 8.0.6 (Hypercube Inc.). The compounds formulae were entered into the data set as two-dimensional

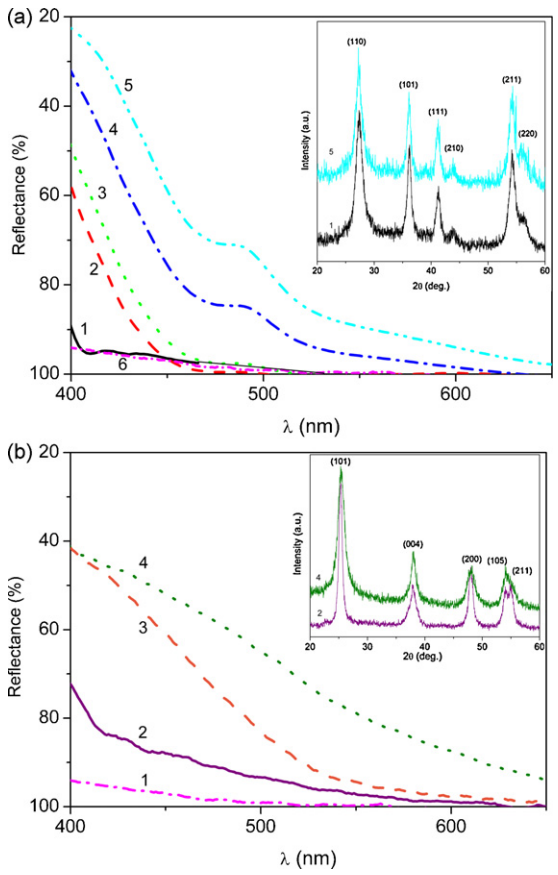

Fig. 2. Diffuse reflectance spectra of the catalysts: (a) 1, rutile TiO_2; 2, TiO_2 + 0.13 at.% Fe; 3, TiO_2 + 0.19 at.% Fe; 4, TiO_2 + 1.27 at.% Fe; 5, TiO_2 + 1.48 at.% Fe; 6, TiO_2 Degussa P25; and (b) 1, TiO_2 Degussa P25; 2, anatase TiO_2; 3, N1-TiO_2; 4, N2-TiO_2. Insets: typical XRD patterns.

sketches into Hyperchem and stored as atomic coordinates. Full optimization geometry and calculation of the positive and negative MEPs for the best conformer were performed using the semi-empirical method AM1 running on Hyperchem. Electronic properties were computed from single point calculations.

3. Results and discussion

3.1. Characteristics of photocatalysts

The influence of doping on the UV/vis spectral properties of TiO_2 is clearly shown in Fig. 2. The DRS of Fe-doped rutile TiO_2 are presented in Fig. 2a and of N-doped anatase TiO_2 in Fig. 2b. As can be seen, the absorption edge of the doped TiO_2 samples shifts toward higher wavelengths, indicating a decrease in the band gap. The reflectance of undoped TiO_2 (Fig. 2a curve 1 and b curve 2) starts to decrease from around ≤420 nm, while the decrease in the reflection of doped samples is significantly shifted to the visible spectral region, as is shown in Table 1. Results of XRD measurements of catalysts are presented as insets in Fig. 2: Fe-doped samples have a rutile crystal structure and N-doped samples have anatase crystal structure, without any detectable dopant-related phase. Average particle diameters calculated from the XRD measurements are presented in Table 1.

Table 1
Absorption thresholds (λ)/band gap energy (E_g) and average particle diameters (D) of applied photocatalysts.

Type of photocatalyst	λ (nm)/E_g (eV)	D (nm)
TiO_2 Degussa P25	~400/3.1	20
Rutile TiO_2	~420/3.0	5–7 [11]
Fe-doped rutile TiO_2	440–550/2.8–2.2	5–7 [11]
Anatase TiO_2	~400/3.2	6–8 [10]
N-doped anatase TiO_2	540–590/2.3–2.1	6–8 [10]

Table 2
Concentration of Fe^{3+} in doped rutile TiO_2 powders.

Sample (% Fe–TiO_2)	Fe at.% (EDS)
Rutile TiO_2	0.00
2.5	0.13
5.0	0.19
10.0	1.27
20.0	1.48

The SEM/EDS measurements showed that the real concentrations of Fe^{3+} in the TiO_2 matrix were much lower than the corresponding stoichiometric values (Table 2), which is in good agreement with the results obtained by the inductively coupled plasma (ICP) method [11].

3.2. Photocatalytic activity of Fe-doped rutile TiO_2

The results of studying the photocatalytic activity of rutile TiO_2 doped with different amounts of Fe^{3+} are presented in Fig. 3. As can be seen, the rate of MCPP degradation in the presence of these catalysts was lower compared to that observed in the presence of undoped rutile (Fig. 3a). Also, the increase in the Fe^{3+} concentration from 0.13 to 1.48 at.% resulted in a decrease of the rate of photocatalytic degradation of MCPP.

In the case of MCPA as substrate, the situation was somewhat different (Fig. 3b). Although the degradation rate in this case was also highest in the presence of undoped rutile TiO_2, the increase in the Fe^{3+} concentration up to 1.27 at.% yielded a slight increase in the degradation rate, followed by a marked decrease with a further increase in the dopant content.

In order to investigate how molecular structure of the substrate influences the rate of its degradation, we compared the processes for MCPP and MCPA, having an aromatic ring in their molecules, with that of CP, whose molecule contains a pyridine ring which has the properties of a strong Lewis base (Fig. 1). It was found that in the case of CP the presence of Fe^{3+} in rutile had a favorable effect on the photocatalyst efficiency, i.e. the increase in the Fe^{3+} content accelerated the CP degradation, as is shown in Fig. 3c.

In view of the fact that the degradation intermediates of MCPP, MCPA and CP might absorb at the same wavelength as the main compound, we applied the LC–DAD technique to separately identify the degradation intermediates and the parent compound. By this technique, we studied the behavior of those Fe-doped rutile TiO_2 catalysts for which spectrophotometric measurements showed the highest photocatalytic efficiency in the case of all three herbicides. Since TiO_2 doped with 0.13 at.% Fe appeared to be most efficient of the synthesized photocatalysts used in the degradation of MCPP and MCPA, the degradation efficiency of these herbicides was studied in the presence of this catalyst (Fig. 4). It was found that the degradation rate of both herbicides was higher than that measured by spectrophotometric method (Fig. 3a and b), which indicates the presence of intermediates. Namely, with both herbicides, the presence of the intermediate 4-chloro-2-methylphenol was observed at the retention time of 4.9 min (Fig. 5, chromatograms 1 and 2), which is in agreement with our previous findings [18,19]. Also, it was found that the rates of degradation of MCPP and MCPA were similar, which is understandable because of the similarity of their structural formulae and physical properties. Since the rate of CP photodegradation determined spectrophotometrically was highest in the presence of TiO_2 doped with 1.27 at.% Fe, the correspond-

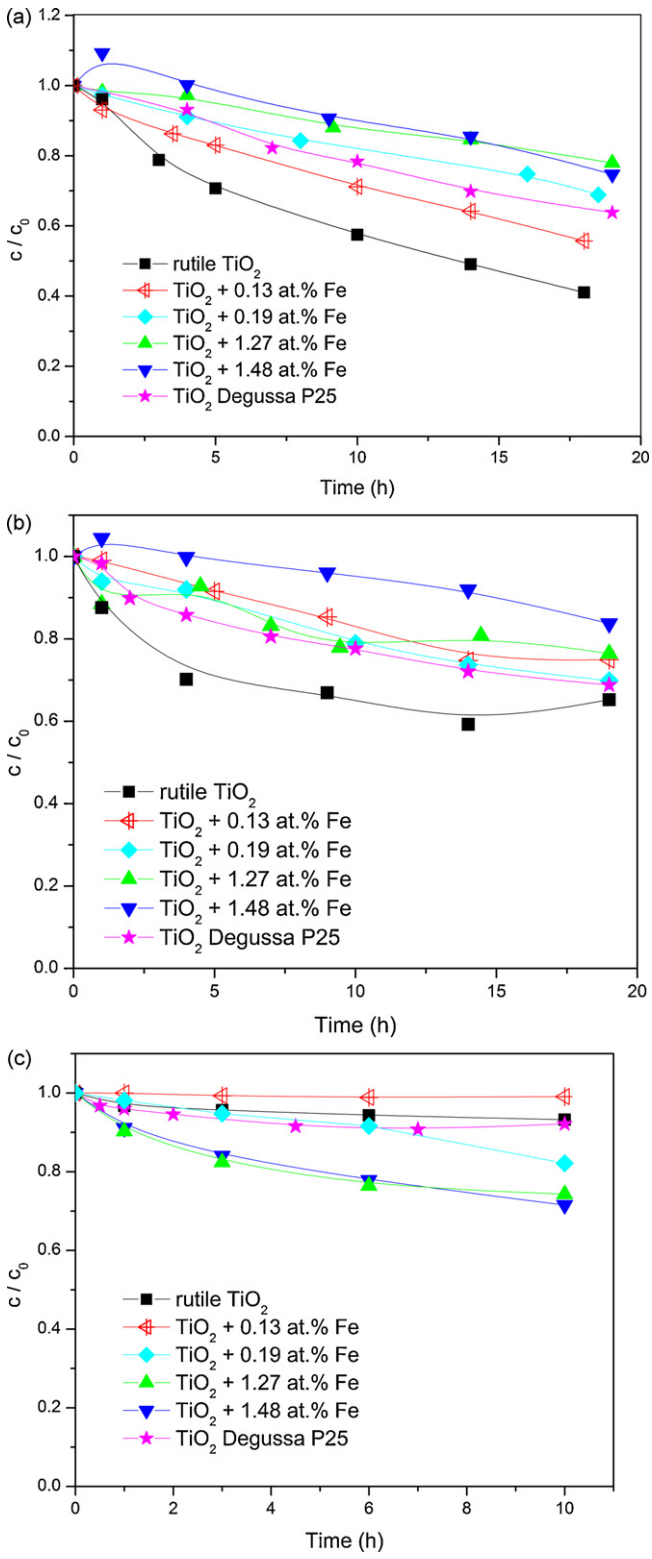

Fig. 3. Spectrophotometric monitoring of herbicides photocatalytic degradation in the presence of rutile TiO_2, rutile TiO_2 doped with different at.% of Fe^{3+} and TiO_2 Degussa P25: (a) MCPP; (b) MCPA; and (c) CP.

ing kinetic curve is also shown in Fig. 4. As can be seen, the rates of CP degradation measured by both techniques are very similar (Figs. 3c and 4), which indicates the absence of intermediates (Fig. 5, chromatogram 3).

The efficiency of the photodegradation processes was compared with that of the direct photolysis performed also using visible light

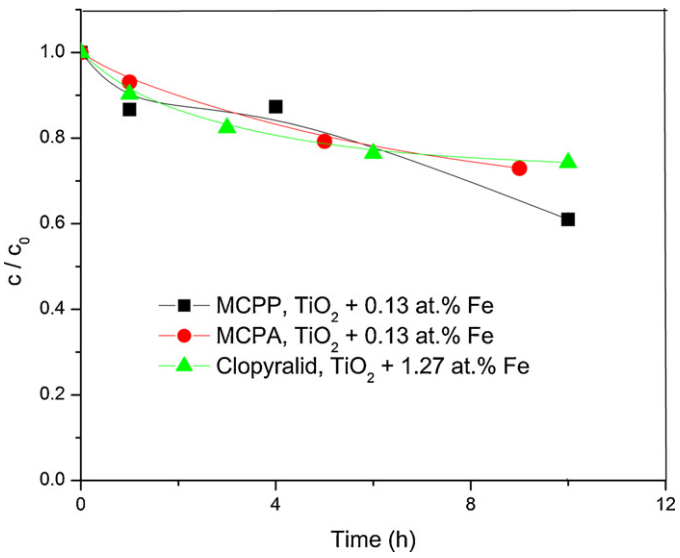

Fig. 4. Kinetics of photocatalytic degradation of herbicides in the presence of Fe-doped rutile TiO_2.

[13,20]. The degradation of all herbicides was detected, but at a much lower rate than in the presence of catalysts, the difference being especially pronounced in the case of MCPP and MCPA. Therefore, it can be concluded that the direct photolysis did not play a significant role in the overall photocatalytic degradation.

To interpret the influence of the presence and concentration of Fe^{3+} ions on the photocatalytic activity of the Fe-doped rutile TiO_2 it is necessary to take into account a number of factors [2]. Firstly, Fe^{3+} ions can enhance the intensity of absorption in the UV/vis light region and make a red shift in the band gap transition of the Fe-doped rutile TiO_2 samples (Fig. 2). This can induce more photogenerated electrons and holes to participate in the photocatalytic reactions. Apart from this effect, Fe^{3+} ions can also serve as a mediator of the transfer of interfacial charges at an appropriate doping concentration. Besides, the presence of a small amount of Fe^{3+} ions can enhance the activity, but excessive Fe^{3+} ions are detrimental [2]. A most probable explanation of the decrease of photocatalytic efficiency with increase in the Fe^{3+} content might be the trapping of holes on the catalyst surface, which lowers their apparent mobility and results in an increased probability of their recombination with electrons [4]. Also, the increase in the Fe^{3+} concentration may lead to the formation of the aggregates of Fe-oxides (Fe_2O_3 or FeO), causing a further decrease of the photodegradation rate, which is a consequence of lower mobility of the charges and reduced adsorp-

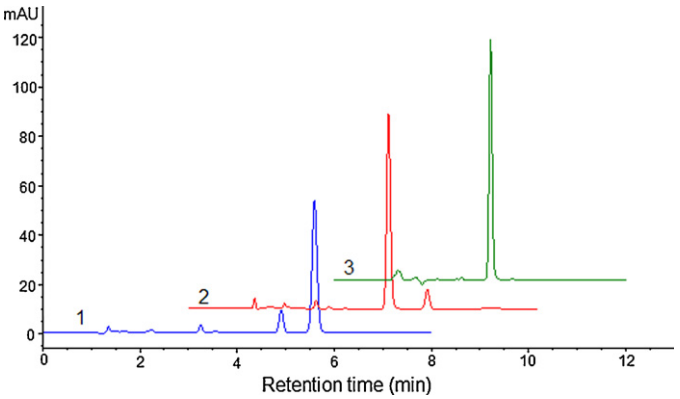

Fig. 5. Chromatograms obtained in the presence of Fe-doped rutile TiO_2 after about 5 h of degradation: (1) MCPP, 0.13 at.% Fe; (2) MCPA, 0.13 at.% Fe; (3) CP, 1.27 at.% Fe.

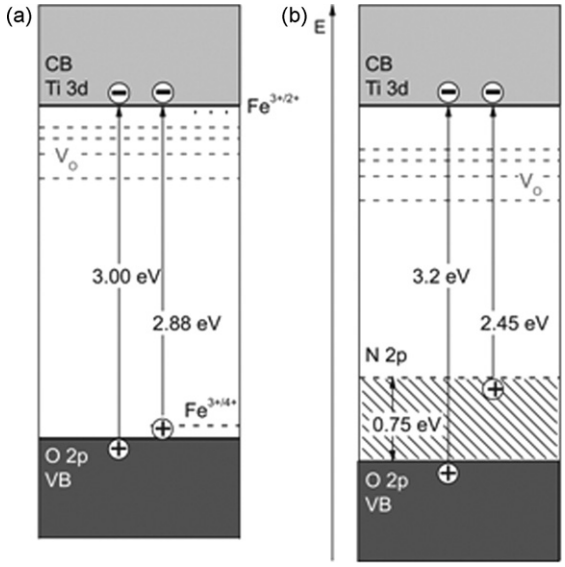

Fig. 6. Relative position of energy levels in photocatalysts: (a) rutile TiO_2 and Fe-doped rutile TiO_2; and (b) anatase TiO_2 and N-doped anatase TiO_2 [29–31].

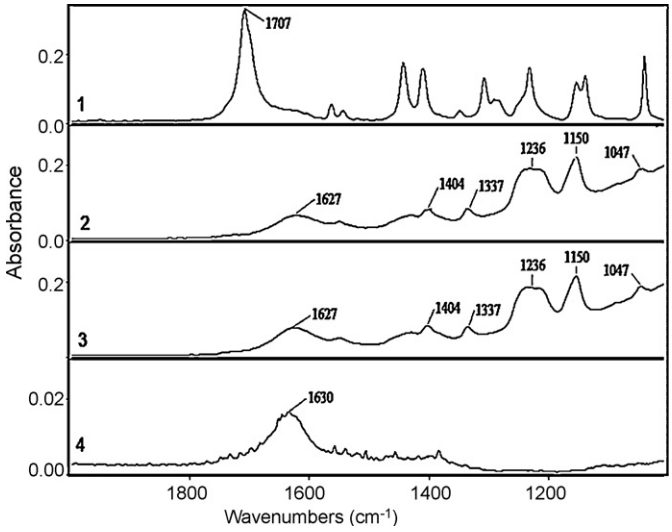

Fig. 7. FTIR spectra of: (1) CP alone; (2) the difference between the spectra of CP adsorbed on TiO_2 Degussa P25 and TiO_2 Degussa P25; (3) CP adsorbed on TiO_2 Degussa P25; (4) TiO_2 Degussa P25.

tive properties of Fe oxide compared to TiO_2 [21]. Secondly, the large surface area may be an important factor in certain photocatalytic degradation reactions, since the large amount of adsorbed organic molecules promotes the reaction rate. However, powders with a large surface area are usually associated with large amounts of crystalline defects which favor the recombination of photogenerated electrons and holes, leading to a poor photoactivity [2]. Thirdly, particle size is another important parameter influencing the photocatalytic efficiency, since the electron–hole recombination rate may depend on the particle size. Finally, but not the least important, come the effects of the substrate structure and the pH at which the photodegradation process is taking place.

The observation that there does not exist an Fe^{3+} concentration at which the photodegradation rate of all tested herbicides would be the highest suggests that the structure of the substrate plays a decisive role in the photocatalytic process. This conclusion is also supported by the finding that the concentrations of MCPP and MCPA on the catalyst with highest Fe^{3+} content (1.48 at.%) in the first period of photocatalytic degradation are higher than their initial equilibrium concentrations (Fig. 3), which may be ascribed to the desorption of the herbicides, induced by irradiation [22]. It is well known that the surface of TiO_2 is amphotheric, so that at a low pH a significant number of surface sites are protonated, yielding a positively charged surface. Hence, the maximum adsorption of carboxylic acids will occur at the pH corresponding to the positively charged TiO_2 surface, as the deprotonated acid molecules carry negative charges. Therefore, one can expect efficient adsorption of acids whose pK_a values (MCPP, $pK_a = 3.11 - 3.78$ [23]; MCPA, $pK_a = 3.1$ [24]; and CP $pK_1 = 1.4$ and $pK_2 = 4.4$ [25]) are lower than the pH_{ZPC} (~5.1) of rutile TiO_2 [26]. Also, FTIR measurements [12,13] confirmed the formation of RS-2-(4-chloro-o-tolyloxy)propionate species after the adsorption of MCPP on the TiO_2 surface. It is obvious that at such high dopant concentration the population of Fe^{3+} ions on the very surface of TiO_2 particles or adjacent to it is relatively high. When the suspension is illuminated, the electrons generated are being rapidly trapped ($Fe^{3+} + e^- \rightarrow Fe^{2+}$) according to Fig. 6a, which affects the surface properties and yields desorption of MCPA and MCPP. As a consequence, an increase in the concentration of the free herbicide in the solution is observed at the beginning of the photocatalytic experiment. Later on, the degradation becomes more intensive than desorption. This effect was not observed with CP, which is a carboxy-pyridine compound, capable to compensate for the disturbance occurring after the irradiation through zwitterion formation [27]. Fig. 7 shows the FTIR spectra of CP itself (curve 1), the difference between the spectra of CP adsorbed on TiO_2 Degussa P25 and TiO_2 Degussa P25 (curve 2), CP adsorbed on TiO_2 Degussa P25 (curve 3), and TiO_2 Degussa P25 (curve 4). Curve 1 has a broad band at 1707 cm^{-1}, corresponding to the C=O vibrations of carboxyl group, substituted in the spectrum of the adsorption product (curves 2 and 3) by the bands of carboxylate anion at 1627, 1404 and 1337 cm^{-1}. These bands are attributed to the newly formed 3,6-dichloropicolinate species. There are also bands at 1047 and 1150 cm^{-1} that are due to the stretching and deformation vibrations of the C—H of the pyridine ring, respectively, and a broad band at 1236 cm^{-1} due to the vibration of the aromatic C—N bond [28]. Significant broadening of the band that corresponds to C—N vibrations can be an indication of the ability of CP to bind through the N atom to the TiO_2 surface.

3.3. Photocatalytic activity of N-doped anatase TiO_2

The LC–DAD measurements served to evaluate photocatalytic activity of the N-doped anatase TiO_2 catalysts in the degradation of all three herbicides. In the case of MCPP (Fig. 8a), these catalysts showed a significantly higher activity compared to that of anatase TiO_2 itself, especially in the initial period of photodegradation. When the substrates were MCPA and CP (Fig. 8b and c), the results were somewhat different. In both cases, the N-doped anatase TiO_2 catalysts exhibited only a slightly higher efficiency, confirming the known fact that photocatalytic activity depends on the type of the substrate. It should be noted that under the given experimental conditions CP degraded only to a very small extent (Fig. 8c).

As can be seen from Fig. 8, the efficiency of N-doped anatase TiO_2 catalysts is almost independent of the stoichiometric ratio of TiO_2 and nitrogen used in their preparation. Namely, the N-doped anatase TiO_2 catalysts were prepared by mixing the dry $Ti(OH)_4$ powder with urea in the ratios 1:1 and 1:2. The obtained results can be explained by the assumption that the photocatalysis takes place mostly on the anatase TiO_2 itself, which also makes the major part of the doped material. The differences in the DRS of the two N-doped titania materials can be explained by the presence of oxygen vacancies, whose concentration increases whenever the dopant ions are introduced into the titania (V_o levels in Fig. 6b). Besides, as

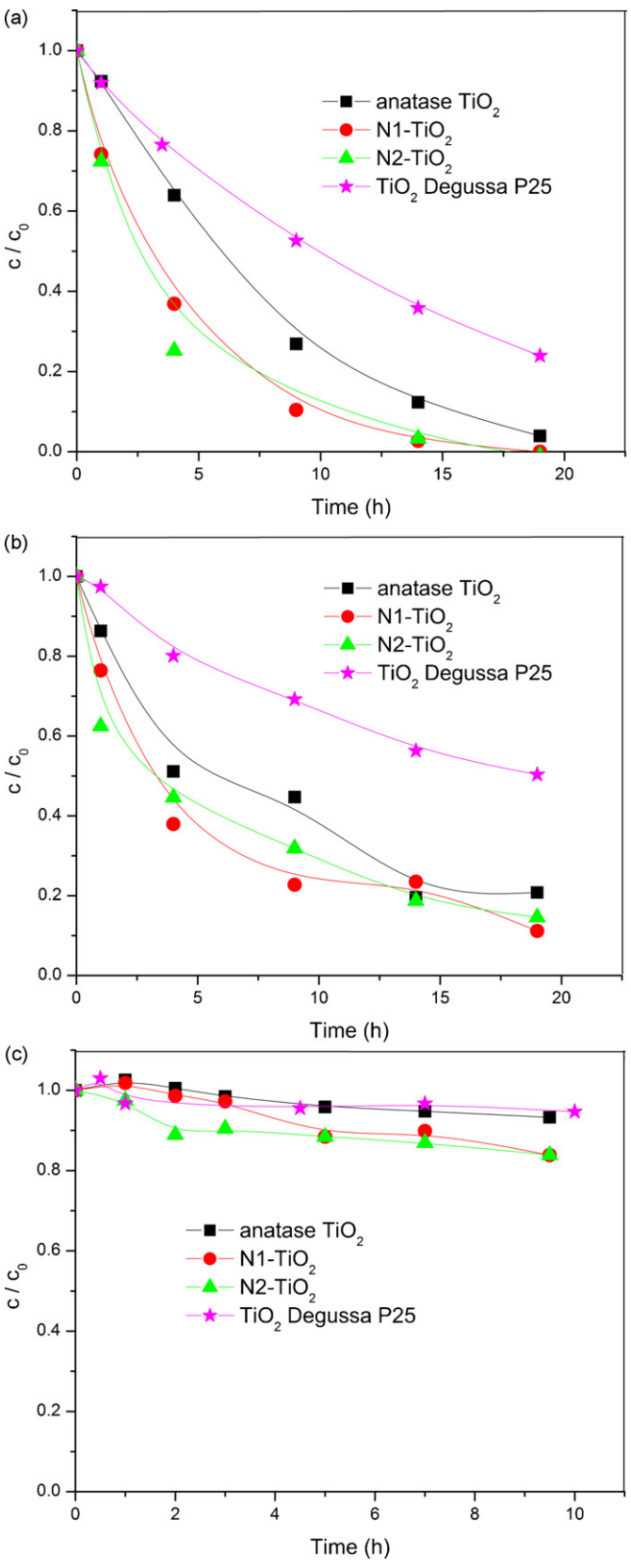

Fig. 8. Kinetics of photocatalytic degradation in the presence of anatase TiO_2, N-doped anatase TiO_2 and TiO_2 Degussa P25: (a) MCPP; (b) MCPA; and (c) CP.

already mentioned, the nitrogen content in the doped catalysts is very small, i.e. it is below the detection limit of the XPS method.

The photocatalytic degradation of all three herbicides was slower on TiO_2 Degussa P25 compared to that on anatase TiO_2 and N-doped anatase TiO_2, which was especially pronounced in the case of MCPP and MCPA. Besides, the smaller size of the anatase TiO_2 and N-doped anatase TiO_2 particles contributes to their higher photocatalytic activity compared to TiO_2 Degussa P25. The increased surface area available for the adsorption of herbicide molecules means at the same time an increase in the population of active sites on which the degradation process takes place. Besides, it should be borne in mind that the recombination of photogenerated e^-–h^+ pairs in the nano-particles is significantly slower compared to the diffusion of free charge carriers to the surface, which contributes to a higher photocatalytic efficiency [32].

3.4. Catalyst's activity and molecular structure of herbicides

On the basis of all the above discussion we can conclude that the differences in photoreactivity are directly related to the electron-donor or electron-withdrawing character of the different substituents in the herbicide aromatic/pyridine ring, which can activate/deactivate the ring with respect to the electrophilic attack of the $^{\bullet}OH$ radical. This may be explained in terms of the effect of Cl and CH_3 group as substituents. Namely, the higher reactivity of MCPP and MCPA compared to CP is probably due to the presence of the benzene-ring activating CH_3 group (Fig. 1). The MCPP and MCPA molecules contain also Cl atoms, playing a deactivating role. However, the CP molecule, although containing a pyridine ring that exhibits properties of a strong Lewis base due to the presence of the nitrogen atom with a lone pair of electrons, which is under the given reaction conditions protonated, has also two Cl atoms bound to the pyridine moiety, causing its lower reactivity compared to that of the other two herbicides. These results are in agreement with those reported in the literature [33]. Also, it is known that pyridine, because of the presence of N atom in its ring, is less reactive than benzene, which also contributes to the lower reactivity of CP compared to MCPP and MCPA. Besides, the presence of the electronegative COO^- group, clearly shown in the Hyperchem-derived MEPs (Fig. 9), indicates that the bond between the substrate and the catalyst is realized via the COO^- group in the case of all three herbicides, since the pH of the suspension is about 3, which renders the catalyst surface positively charged. Fig. 9 shows that the negative electrostatic potential on the COO^- group of MCPA and MCPP is lower compared to that of CP, this property being directly proportional to the photoreactivity of the herbicide molecule.

The herbicides adsorption on TiO_2 Degussa P25 was also assessed in order to determine how herbicide structure influences the adsorption on the catalyst. It appeared that the adsorption after 15-min sonication of CP suspension was very low (about 3%), the adsorption of MCPP and MCPA being somewhat more pronounced (about 6%). This is directly proportional to the photocatalytic degradation rate of these herbicides and may be still another explanation for the slower reaction of CP compared to MCPP and MCPA.

In summary, the results indicated that the rate of MCPP and MCPA degradation is higher on undoped rutile TiO_2 photocatalyst compared to its Fe-doped form. Contrary, the degradation of CP on undoped rutile TiO_2 is less efficient than on the Fe-doped catalyst, the only exception being the catalyst with the lowest iron content (0.13 at.%). A comparison of the performance of undoped rutile TiO_2 and Fe-doped rutile TiO_2 with that of TiO_2 Degussa P25 shows that rutile TiO_2 is more efficient in the degradation of MCPP and MCPA, the efficiency of the Fe-doped rutile TiO_2 being similar to or lower than that of TiO_2 Degussa P25. The efficiency of the former two catalysts in CP degradation is also similar to or higher than that of TiO_2 Degussa P25. The N-doped anatase TiO_2 is more efficient than

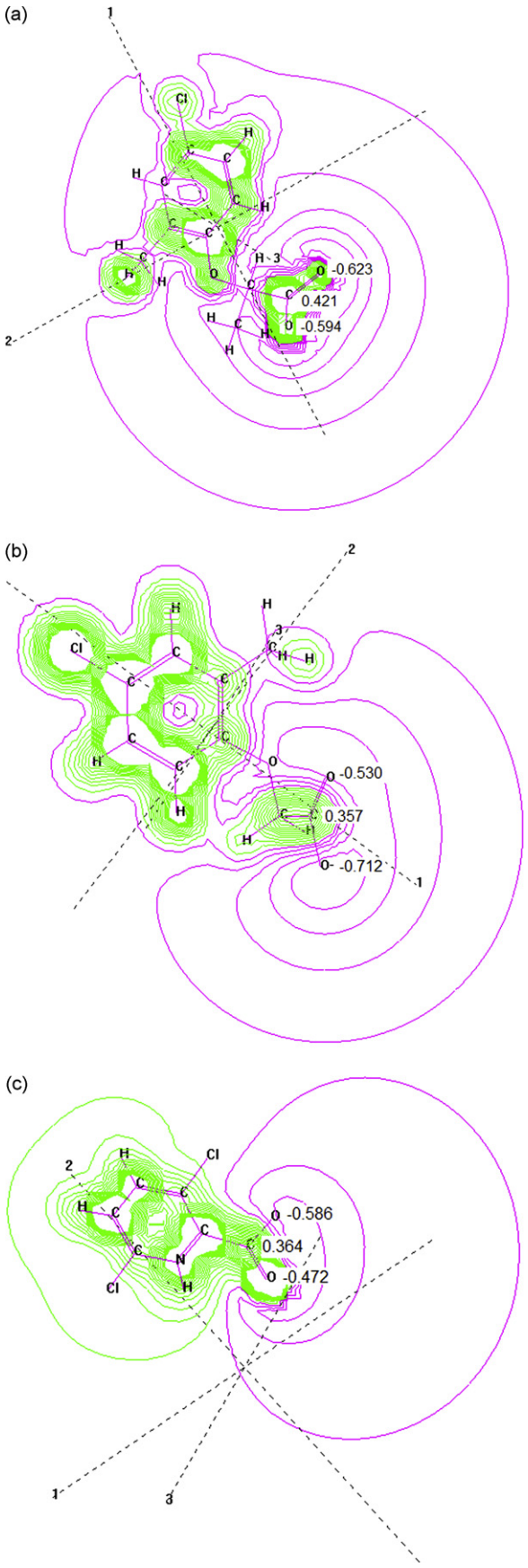

Fig. 9. MEP maps for the herbicide molecules. Electronegative and electropositive potential contours are shown in red and green lines, respectively: (a) MCPP; (b) MCPA; and (c) CP.

undoped anatase TiO_2 in the photocatalytic degradation of MCPP and MCPA, the increase in the efficiency being more pronounced in the case of MCPA. However, the N-doped anatase TiO_2 is inefficient in the degradation of CP, indicating that the photocatalytic activity depends on the structure of the substrate. A comparison of the efficiency of the N-doped anatase TiO_2 with that of Fe-doped rutile TiO_2 shows that the former is advantageous, confirming the observation that non-metals are more efficient dopants than metals. Finally, a comparison of the photocatalytic efficiency of the two crystalline forms of TiO_2, rutile and anatase, shows that the latter is more active in the case of all three herbicides, which can be explained by a higher mobility of free charge carriers in anatase.

4. Conclusion

The results showed that all investigated herbicides can be photocatalytically decomposed in the presence of Fe- or N-doped TiO_2, under visible light irradiation. Doping of rutile TiO_2 with Fe^{3+} lowered its photocatalytic activity in the case of MCPP and MCPA degradation. In contrast to this, the rate of CP degradation increased with increase in the Fe^{3+} content up to 1.27 at.%. When N-doped anatase TiO_2 was used, the rate of degradation of all three herbicides was higher compared to that obtained using undoped anatase TiO_2, the effect being most pronounced in the photodegradation of MCPP. In all the cases the photocatalytic efficiency of undoped anatase TiO_2 was higher compared to that of the undoped rutile form. Results indicate that the efficiency of photocatalytic degradation is greatly influenced by the molecular structure of the compound. Lowering of the band gap of titanium dioxide by doping is not always favorable for increasing photocatalytic efficacy of degradation.

Acknowledgments

This work was financially supported by the Ministry of Science and Technological Development of the Republic of Serbia (Projects No. ON142029 and ON142066) and Provincial Secretariat for Science and Technological Development, Novi Sad (Grant No. 114-451-00704/2008-01).

References

[1] D. Chatterjee, S. Dasgupta, Visible light induced photocatalytic degradation of organic pollutants, J. Photochem. Photobiol. C: Photochem. Rev. 6 (2005) 186–205.
[2] M. Zhou, J. Yu, B. Cheng, Effects of Fe-doping on the photocatalytic activity of mesoporous TiO_2 powders prepared by an ultrasonic method, J. Hazard. Mater. 137 (2006) 1838–1847.
[3] J.A. Navío, F.J. Marchena, M. Roncel, M.A. De La Rosa, A laser flash photolysis study of the reduction of methyl viologen by conduction band electrons of TiO_2 and Fe–Ti oxide photocatalysts, J. Photochem. Photobiol. A: Chem. 55 (1991) 319–322.
[4] Z.B. Zhang, C.C. Wang, R. Zakaria, J.Y. Ying, Role of particle size in nanocrystalline TiO_2-based photocatalysts, J. Phys. Chem. B 102 (1998) 10871–10878.
[5] S.U.M. Khan, M. Al-Shahry, W.B. Ingler Jr., Efficient photochemical water splitting by a chemically modified n-TiO_2, Science 297 (2002) 2243–2245.
[6] T. Umebayashi, T. Yamaki, H. Itoh, K. Asai, Band gap narrowing of titanium dioxide by sulfur doping, Appl. Phys. Lett. 81 (2002) 454–456.
[7] L. Lin, W. Lin, Y. Zhu, B. Zhao, Y. Xie, Phosphor-doped titania—a novel photocatalyst active in visible light, Chem. Lett. 34 (2005) 284–285.
[8] J.C. Yu, J. Yu, W. Ho, Z. Jiang, L. Zhang, Effects of F^- doping on the photocatalytic activity and microstructures of nanocrystalline TiO_2 powders, Chem. Mater. 14 (2002) 3808–3816.
[9] C. Di Valentin, E. Finazzi, G. Pacchioni, A. Selloni, S. Livraghi, M.C. Paganini, E. Giamello, N-doped TiO_2: theory and experiment, Chem. Phys. 339 (2007) 44–56.
[10] N.D. Abazović, A. Montone, L. Mirenghi, I.A. Janković, M.I. Čomor, TiO_2 doped with nitrogen: synthesis and characterization, J. Nanosci. Nanotechnol. 8 (2008) 613–618.
[11] N.D. Abazović, L. Mirenghi, I.A. Janković, N. Bibić, D.V. Šojić, B.F. Abramović, M.I. Čomor, Synthesis and characterization of rutile TiO_2 nanopowders doped with iron ions, Nanoscale Res. Lett. 4 (2009) 518–525.

[12] B. Abramović, D. Šojić, V. Anderluh, Visible-light-induced photocatalytic degradation of herbicide mecoprop in aqueous suspension of TiO_2, Acta Chim. Slov. 54 (2007) 558–564.
[13] B.F. Abramović, D.V. Šojić, V.B. Anderluh, N.D. Abazović, M.I. Čomor, Nitrogen-doped TiO_2 suspensions in photocatalytic degradation of herbicides mecoprop and (4-chloro-2-methylphenoxy)acetic acid using various light sources, Desalination 244 (2009) 293–302.
[14] N. Gray (Ed.), Pesticides and Organic Micropollutants, Drinking Water Quality, John Wiley & Sons, Chichester, 1996, pp. 132–148.
[15] D.B. Donald, A.J. Cessna, E. Sverko, N.E. Glozier, Pesticides in surface drinking-water supplies of the northern Great Plains, Environ. Health Perspect. 115 (2007) 1183–1191.
[16] H. Irie, Y. Watanabe, K. Hashimoto, Nitrogen-concentration dependence on photocatalytic activity of $TiO_{2-x}N_x$ powders, J. Phys. Chem. B 107 (2003) 5483–5486.
[17] K. Kobayakawa, Y. Murakami, Y. Sato, Visible-light active N-doped TiO_2 prepared by heating of titanium hydroxide and urea, J. Photochem. Photobiol. A: Chem. 170 (2005) 177–179.
[18] A. Topalov, D. Molnár-Gábor, M. Kosanić, B. Abramović, Photomineralization of the herbicide mecoprop dissolved in water sensitized by TiO_2, Water Res. 34 (2000) 1473–1478.
[19] A. Topalov, B. Abramović, D. Molnár-Gábor, J. Csanádi, O. Arcson, Photocatalytic oxidation of the herbicide (4-chloro-2-methylphenoxy)acetic acid (MCPA) over TiO_2, J. Photochem. Photobiol. A: Chem. 140 (2001) 249–253.
[20] B. Abramović, V. Anderluh, D. Šojić, F. Gaál, Photocatalytic removal of herbicide clopyralid from water, J. Serb. Chem. Soc. 72 (2007) 1477–1486.
[21] D.W. Bahnemann, Ultrasmall metal oxides: preparation, photophysical characterization and photocatalytic properties, Isr. J. Chem. 33 (1993) 115–136.
[22] J. Zhu, F. Chen, J. Zhang, H. Chen, M. Anpo, Fe^{3+}–TiO_2 photocatalysts prepared by combining sol–gel method with hydrothermal treatment and their characterization, J. Photochem. Photobiol. A: Chem. 180 (2006) 196–204.
[23] L. Clausen, I. Fabricius, Atrazine, isoproturon, mecoprop, 2,4-D, and bentazone adsorption onto iron oxides, J. Environ. Qual. 30 (2001) 858–869.
[24] C.D.S. Tomlin (Ed.), The Pesticide Manual, 11th ed., The British Crop Protection Council, The Bath Press, Bath, UK, 1997.
[25] M.C. Corredor, J.M. Rodríguez Mellado, M. Ruiz Montoya, EC(EE) process in the reduction of the herbicide clopyralid on mercury electrodes, Electrochim. Acta 51 (2006) 4302–4308.
[26] M.L. Machesky, D.J. Wesolowski, D.A. Palmer, K. Ichiro-Hayashi, Potentiometric titrations of rutile suspensions to 250 °C, J. Colloid Interface Sci. 200 (1998) 298–309.
[27] D.V. Šojić, V.B. Anderluh, D.Z. Orčić, B.F. Abramović, Photodegradation of clopyralid in TiO_2 suspensions: identification of intermediates and reaction pathways, J. Hazard. Mater. 168 (2009) 94–101.
[28] I. Pavlović, C. Barriga, M.C. Hermosín, J. Cornejo, M.A. Ulibarri, Adsorption of acidic pesticides 2,4-D, clopyralid and picloram on calcined hydrotalcite, Appl. Clay Sci. 30 (2005) 125–133.
[29] N.D. Abazović, M.I. Čomor, M.D. Dramićanin, D.J. Jovanović, P.S. Ahrenkiel, J.M. Nedeljković, Photoluminescence of anatase and rutile TiO_2 particles, J. Phys. Chem. B 110 (2006) 25366–25370 (and references therein).
[30] R. Nakamura, T. Tanaka, Y. Nakato, Mechanism for visible light responses in anodic photocurrents at N-doped TiO_2 film electrodes, J. Phys. Chem. B 108 (2004) 10617–10620.
[31] C. Wang, C. Böttcher, D.W. Bahnemann, J.K. Dohrmann, A comparative study of nanometer sized Fe(III)-doped TiO_2 photocatalysts: synthesis, characterization and activity, J. Mater. Chem. 13 (2003) 2322–2329.
[32] D.F. Ollis, N. Pelizzetti, N. Serpone, in: N. Serpone, E. Pelizzetti (Eds.), Photocatalysis. Fundamentals and Applications, John Wiley & Sons, New York, 1989.
[33] S. Parra, J. Olivero, C. Pulgarin, Relationships between physicochemical properties and photoreactivity of four biorecalcitrant phenylurea herbicides in aqueous TiO_2 suspension, Appl. Catal. B: Environ. 36 (2002) 75–85.